Molecular Cell, Volume *76*

Supplemental Information

mTORC1 Activation Requires DRAM-1 by Facilitating Lysosomal Amino Acid Efflux

Florian Beaumatin, Jim O'Prey, Valentin J.A. Barthet, Barbara Zunino, Jean-Philippe Parvy, Alexis Maximilien Bachmann, Margaret O'Prey, Elżbieta Kania, Pablo Sierra Gonzalez, Robin Macintosh, Laurence Y. Lao, Colin Nixon, Jonathan Lopez, Jaclyn S. Long, Stephen W.G. Tait, and Kevin M. Ryan

Supplementary Figure Legends

Figure S1. Loss of DRAM-1 affects the rate of autophagy inactivation upon re-feeding, Related to Figure 1.

(A) RNA was extracted from *Dram-1*$^{flox/flox}$ MEF cells infected with retroviruses encoding or not Cre recombinase enzyme. *Dram1* mRNA levels were normalised to 18S mRNA levels and were compared to cells not expressing Cre recombinase (CTL). Data are mean +/-SD. (B) MEF from wild type mice were isolated and immortalized by serial passages prior to being infected with retroviruses encoding or not Cre recombinase enzyme. Cells were then starved in EBSS containing glutamine for 3 h prior to 20 minutes treatment in EBSS supplemented by 0.8 mM leucine. mTOR activation was evaluated by western blot using phospho-S6 kinase, phosho-S6 ribosomal protein and phospho-4E-BP1 antibodies while total S6 kinase, total S6 ribosomal protein, total 4E-BP1 and ERK2 antibodies were used as loading controls. (C) Quantifications of 3 independent experiments shown in figure 1D. LC3-II protein levels were determined using ImageJ software and normalised to ERK2 levels. Data are mean +/-SD. *p <0.05

Figure S2. Loss of autophagy only affects leucine-stimulated mTORC1 activation in the absence of DRAM-1, Related to Figure 1.

(A) MEFs were isolated from E13.5 embryos resulting from the intercross of *Atg7*$^{flox/flox}$ *Dram1*$^{+/-}$ mice and were genotyped by PCR. *Atg7*$^{flox/flox}$ *Dram1*$^{+/+}$ or *Dram1*$^{-/-}$ cells were selected and immortalized by serial passage. (B) *Atg7*$^{flox/flox}$ *Dram1*$^{-/-}$ or *Atg7*$^{flox/flox}$ *Dram1*$^{+/+}$ cells were starved in EBSS containing glutamine for 3 h prior to the stimulation of mTOR by treating cells with EBSS containing 0.8 mM leucine for 20 min. mTOR activation was detected by measuring

phospho-S6 kinase. Total S6 kinase and ERK2 were used as loading controls. (C) *Atg7*$^{flox/flox}$ *Dram1*$^{-/-}$ or *Atg7*$^{flox/flox}$ *Dram1*$^{+/+}$ cells were starved in EBSS containing glutamine for 3 h prior to re-stimulation of mTOR by treating cells with regular DMEM medium for the indicated times. mTOR-induced autophagy inhibition was assessed by western blots directed against phospho-S6 kinase and LC3B antibodies. Total S6 kinase and ERK2 were used as loading controls. (D) Analysis of cell growth of *Atg7*$^{flox/flox}$ *Dram1*$^{-/-}$ or *Atg7*$^{flox/flox}$ *Dram1*$^{+/+}$ cells. Equal amounts of cells were split on day 0 in complete DMEM. From day 2 cells were harvested daily and counted using an Innovatis cell counter. Results shown are representative from 3 independent experiments. Data are mean +/-SEM. * $p < 0.05$. (E) *Atg7*$^{flox/flox}$ *Dram1*$^{-/-}$ or *Atg7*$^{flox/flox}$ *Dram1*$^{+/+}$ cells were starved for 3 h in EBSS containing glutamine with or without 100 nM of Bafilomycin A1 (Baf A1) prior to stimulation of mTOR using EBSS containing 0.8 mM leucine for 20 min. mTOR activation was evaluated by western blots as described above. Lysosomal impairment caused by bafilomycin A1 treatment was controlled by western blot directed against LC3B (I and II). (F) Deletion of *Atg7* was performed by infecting cells with a retrovirus expressing Cre recombinase and verified by western blot against ATG7 and LC3B (as a control for the functional inhibition of the autophagy pathway). (G) DRAM1$^{-/-}$ or DRAM1$^{+/+}$ cells which were either wild-type (fl/fl) or null (-/-) for ATG7 were starved for 3 h in EBSS containing glutamine prior to incubation in presence of leucine for 20 min. (H) Quantification of the levels of phospho-S6 kinase induced by leucine treatments from 3 independent experiments were performed using ImageJ software. Data are mean +/- SEM. * $p < 0.05$.

Figure S3. The C-terminal region of DRAM-1 is required for LAT-1 binding, Related to Figure 2.

(A) Tandem-affinity purification tag (TAP-TAG) experiments were performed in HeLa cells expressing DRAM1-TAP. Peptides from DRAM1 partners were identified by mass spectrometry. Peptides from specific DRAM1 partners that were identified in least one of the 3 independent experiments (#1, #2, #3) are shown in the table. (B) HEK293T cells transiently expressing the indicated constructs were used to perform co-immunoprecipitations using myc-tag antibody. Western blot analysis of myc-tagged proteins was performed to evaluate the efficiency of the immunoprecipitation while western blot analysis of SLC7A5 (LAT1) expression was used to measure the amount of LAT1 specifically bound to the indicated construct. (C) Quantification of LAT1 bound to each construct from 3 independent experiments. LAT1 levels were measured, normalized and compared to the wild-type DRAM1 construct (1-236-myc-tag-GFP) using ImageJ software. ERK2 was used as a loading control. p-value: Data are mean +/-SEM. *p <0.05

Figure S4. DRAM-1 facilitates the localization of amino acid transporters to lysosomes leading to lysosomal amino acid efflux, Related to Figure 3.

(A)*Dram1*$^{flox/flox}$ MEF expressing Cre recombinase (-/-) or a control vector (fl/fl) and stably expressing SLC3A2-GFP-RFP or GFP-RFP-SLC3A2 constructs were grown in complete medium (FED) or starved using EBSS for 3 h (STARV) before harvesting and analysis by flow cytometry. Mean fluorescence intensities (MFI) for GFP and mRFP were determined and results are shown as percentage of GFP/mRFP ratios compared to SLC3A2-GFP-RFP / DRAM1 expressing MEFs grown under complete condition. Results shown are quantifications of 3 independent experiments. *p < 0.05. (B) *Dram1*$^{flox/flox}$ MEFs expressing a SLC3A2-RFP-GFP construct and expressing or not Cre recombinase enzyme were grown 24 h in regular DMEM

medium supplemented with 10% FBS, 2 mM glutamine and Pen/Strep antibiotics. Before analysing SLC3A2-RFP-GFP fluorescent cellular patterns using confocal microscopy, cells were first incubated 30 min in presence of deepRed Lysotracker and washed 3 times in regular DMEM for 10 min. A representative z-stack for GFP, RFP and lysotracker (white) fluorescences is shown for each cell line. Scale bars represent 20μm. (C) Quantification of lysosomal volume per cell and (D) the amount of SLC3A2-GFP-RFP colocalizing with lysosomes were performed with 50 cells per cell lines. ****p <0.0001. (E) Saos2 TetOn-DRAM1 cells stably expressing LAMP1-RFP-Flag2X were used to purify lysosomal fractions. Aliquots from different steps of the purification protocol (PNS: Post-Nuclear Supernatant, S/N: Supernatant, FT: Flow through, Lyso: Lysosomal fraction) were analysed by western blot for subcellular markers: cytosolic fraction (ERK2 and LC3-I), autophagosomal and autolysosomal fractions (LC3-II) and lysosomes (LAMP2 and DRAM1). (F) Intracellular methyl-leucine (CH_3-leucine) content was measured by metabolite extractions from *Dram1*$^{flox/flox}$ MEFs expressing Cre recombinase enzyme (-/-) or a control vector (fl/fl) starved for 3 h in EBSS with glutamine prior to treatment with 0.8 mM methyl-leucine ester in EBSS supplemented or not with 10 mM D-phenylalanine for 20 min. (G) *Slc1a5* and *Slc7a5* knock-down efficiencies were measured following RNA extraction and qPCR analysis from *Dram1*$^{flox/flox}$ MEFs expressing a control vector and transfected with siRNAs against *Slc1a5* or *Slc7a5* or non-targeting control siRNAs. (H) Metabolites were extracted from Saos2 TetOn-DRAM1 lysosomal fractions prior to analysing their glutamine contents using HPLC-MS. Results are presented as the amount of lysosomal glutamine measured for each condition and normalized to non-induced DRAM1 cells treated with methyl-leucine ester. Quantifications are from 3 independent experiments. *p < 0.05 (A,C,D,F) Data are mean +/-SD. (G,H) Data are mean +/-SEM.

Figure S5. Loss of DRAM-1 increases the rate of AKT phosphorylation in response to insulin, Related to Figure 5.

Dram1$^{flox/flox}$ MEFs expressing Cre recombinase enzyme (-/-) or a control vector (fl/fl) were grown over-night in serum depleted DMEM prior to treatment with indicated amounts of insulin for 15 min. Western blots for Phospho-AKT T308 and Phospho-S6 ribosomal protein were performed to evaluate the activation of the insulin pathway. AKT and S6 were used as loading controls.

Figure S6. Loss of DRAM-1 affects insulin sensitivity and signalling *in vivo*, Related to Figure 6.

(A and B) Insulin tolerance test performed on DRAM1 wild-type (A) or knock-out (B) mice fed for 20 weeks a standard chow diet or a high fat diet (HFD) and treated or not by intraperitoneal injection of rapamycin twice a week (10 mice per condition). p-values compared for each time point to chow diet for each genetic background. p* <0.05, p** <0.01 and p*** <0.001. (C) Percentage of liver weight normalised to total mouse weight measured for each mouse after 22 weeks of HFD. (D) Epididymal adipocyte densities were measured by counting numbers of nuclei from H&E staining of IHC pictures. A minimum of 3 pictures per mouse and 5 mice per condition were quantified using Adobe Photoshop CS5.1 software. (E) Epididymal adipocyte sizes were quantified from H&E staining of IHC pictures. A minimum of 3 pictures per mouse and 5 mice per conditions were quantified using ImageJ software. (F-K) phosphorylation levels in epididymal adipose tissues were evaluated by means of western blots directed against Phospho-S6 kinase, Phospho-AKT T308, Phospho-AKT S473, Phospho-S636/639 IRS1, total S6

Kinase, total AKT and total IRS1 antibodies (I-K). Quantifications of Phospho-AKT S473 or T308 and total IRS1 were performed by western blot in 10 different mouse adipose tissues for each group by using ImageJ software for the indicated antibody (F-H). $p^{*} < 0.05$, $p^{**} < 0.01$ and $p^{***} < 0.001$. n.s = non-significant (A-H) Data are mean +/-SEM.

Figure S7. DRAM-1 is induced during adipocyte differentiation, but loss of DRAM-1 does not affect S6K phosphorylation in this context, Related to Figure 7.

(A) DRAM1 expression levels measured following RNA extraction and qPCR analysis from 3T3-L1 NTC CRISPR cells grown with regular or differentiation media containing 40 µM of troglitazone. (B) 3T3-L1 pre-adipocytes transduced with 2 non targeting control single guides (NTC) or 2 single guides targeting mouse *Dram-1* were transfected following calcium/phosphate transfection protocol with a plasmid coding for myc-tagged mouse *Dram1*. 48h post-transfection proteins were extracted and subjected to western blot analysis using anti-myc tag and ERK2 antibodies. (C) S6 Kinase activation levels from 3T3-L1 CRISPR *Dram-1* or NTC differentiated or not were evaluated by western blot and quantified from 3 independent experiments using ImageJ software. (A,C) Data are mean +/-SEM.

Beaumatin_Sup.Fig1

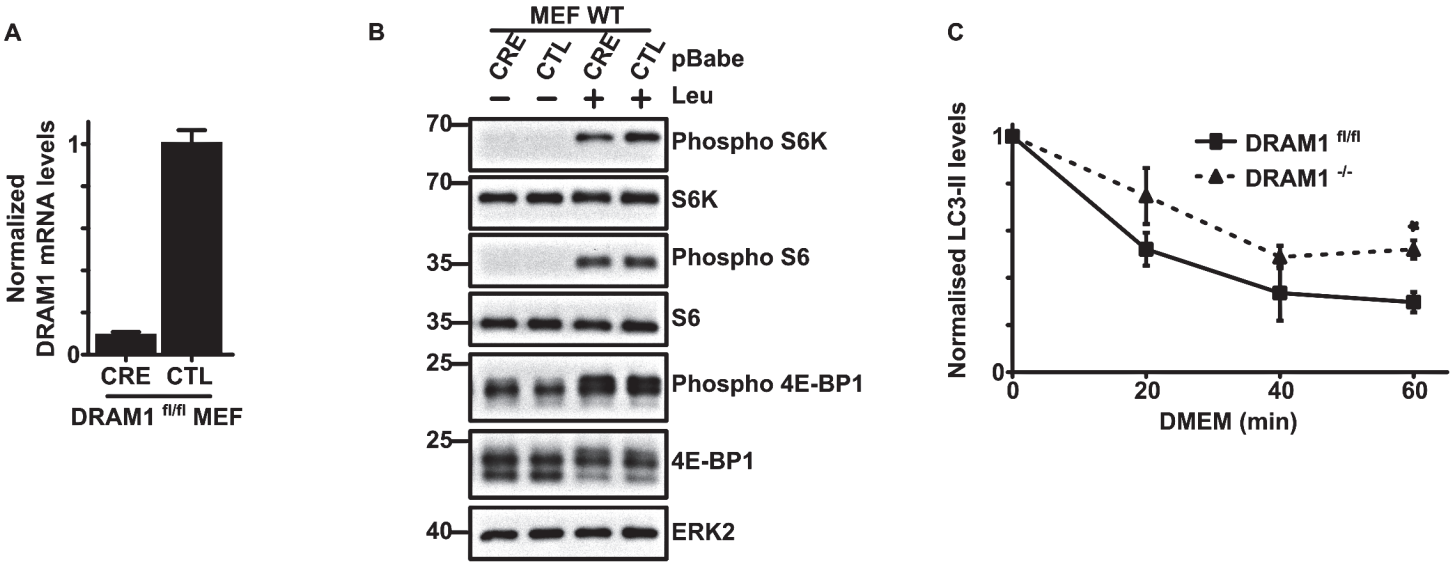

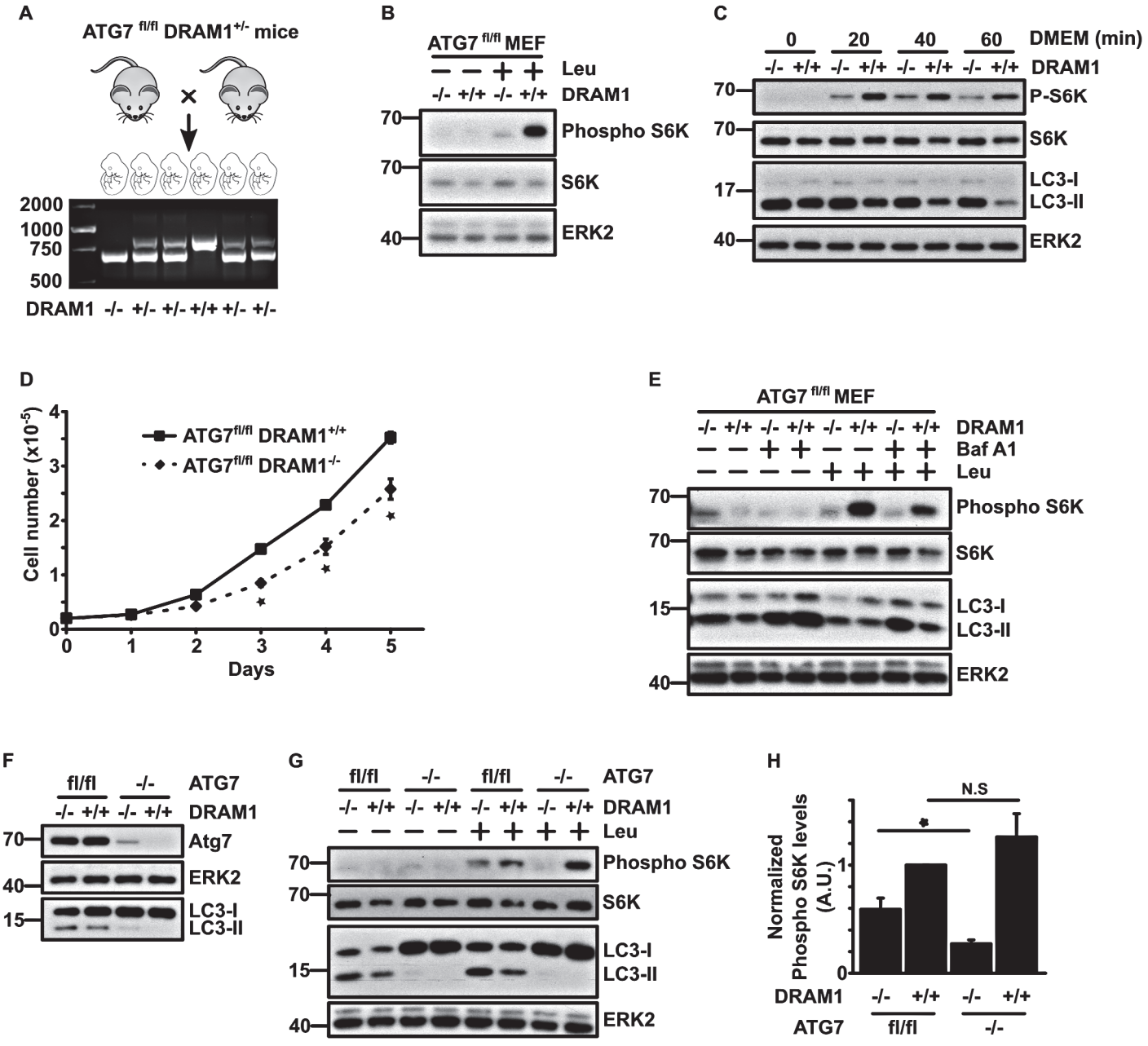
A
ATG7 fl/fl DRAM1+/- mice
2000
1000
750
500
DRAM1 -/- +/- +/- +/+ +/- +/-
B
ATG7 fl/fl MEF
Leu
DRAM1
-/- +/+ -/- +/+
70
Phospho S6K
70
S6K
40
ERK2
C
0 20 40 60 DMEM (min)
DRAM1
-/- +/+ -/- +/+ -/- +/+ -/- +/+
70
P-S6K
70
S6K
17
LC3-I
LC3-II
40
ERK2
D
Cell number (x10-5)
ATG7fl/fl DRAM1+/+
ATG7fl/fl DRAM1-/-
Days
E
ATG7 fl/fl MEF
DRAM1
Baf A1
Leu
70
Phospho S6K
70
S6K
15
LC3-I
LC3-II
40
ERK2
F
fl/fl -/- ATG7
-/- +/+ -/- +/+ DRAM1
70
Atg7
40
ERK2
15
LC3-I
LC3-II
G
fl/fl -/- fl/fl -/- ATG7
-/- +/+ -/- +/+ -/- +/+ -/- +/+ DRAM1
Leu
70
Phospho S6K
70
S6K
15
LC3-I
LC3-II
40
ERK2
H
N.S
*
Normalized Phospho S6K levels (A.U.)
1
0
DRAM1 -/- +/+ -/- +/+
ATG7 fl/fl -/-

Beaumatin_Sup.Fig3

A

Gene name	Description	Peptide nb		
		#1	#2	#3
ATP5B	ATP synthase subunit beta	9	8	8
SLC3A2	4F2 cell-surface antigen heavy chain	7	10	4
SLC1A5	Neutral amino acid transporter B(0)	4	2	1
SLC7A5	Large neutral amino acids transporter small subunit 1	3	2	1
PHB2	Prohibitin-2	4	6	0
ATP5A1	ATP synthase subunit alpha	0	10	7
STOM	Erythrocyte band 7 integral membrane protein	5	0	0
CPS1	Carbamoyl-phosphate synthase	0	5	6
IGJ	Immunoglogulin J chain	3	0	0
OXCT1	Succinyl-CoA:3-ketoacid-coenzyme A transferase 1	0	6	2
PCCB	Propionyl-CoA carboxylase beta chain	0	0	3
GCN1L1	Translational activator GCN1	4	0	0
LMNB1	Lamin-B1	5	0	0
CXCR4	C-X-C chemokine receptor type 4	3	0	0
PIGR	Polymeric immunoglobulin receptor	3	0	0
SLC25A5	ADP/ATP translocase 2	5	2	0
VPS35	Vacuolar protein sorting-associated protein 35	0	4	2
SLC25A3	Phosphate carrier protein	0	3	2
SLC25A13	Calcium-binding mitochondrial carrier protein Aralar 2	0	3	1
TUBB6	Tubulin beta-6 chain	3	0	0
SLC16A3	Monocarboxylate transporter 4	0	2	2
ABCC1	Multidrug resistance-associated protein 1	4	0	0
SPNS1	Protein spinster homolog 1	0	1	2
IGHA1	Ig alpha-1 chain C region	8	0	0
VDAC2	Voltage-dependent anion-selective channel protein 2	0	2	0
FLNA	Filamin-A	0	2	0
PCCA	Propionyl-CoA carboxylase alpha chain	0	0	2
GFM1	Elongation factor G	0	2	0
PHB	Prohibitin	0	2	0
SCAMP3	Secretory carrier-associated membrane protein 3	0	2	0
PKM2	Pyruvate kinase isozymes M1/M2	0	0	2
TMEM55B	Transmembrane protein 55B	0	0	2
SLC35B2	Adenosine 3'-phospho 5'-phosphosulfate transporter 1	0	2	0

B

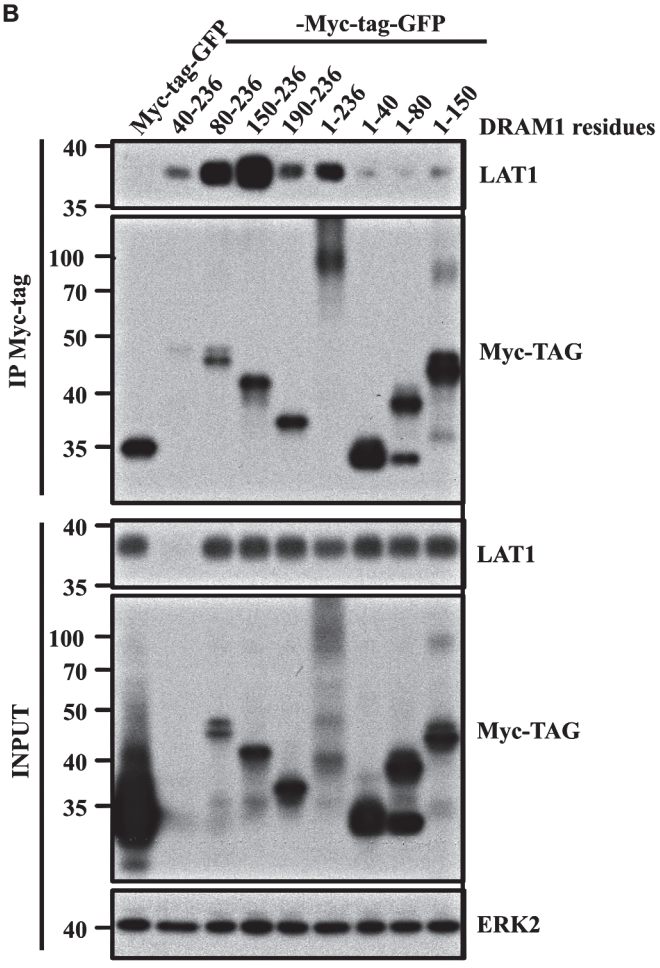

C

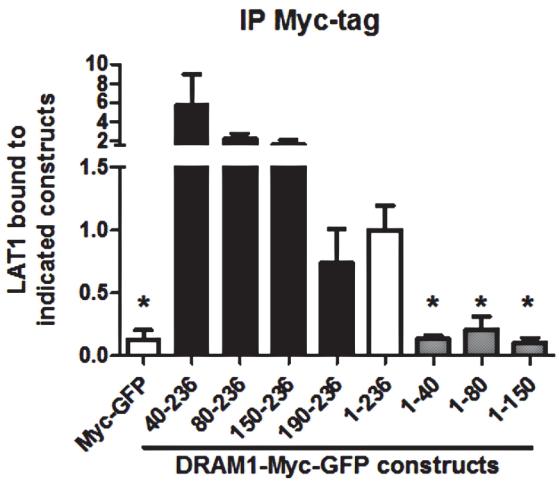

Beaumatin_Sup.Fig4

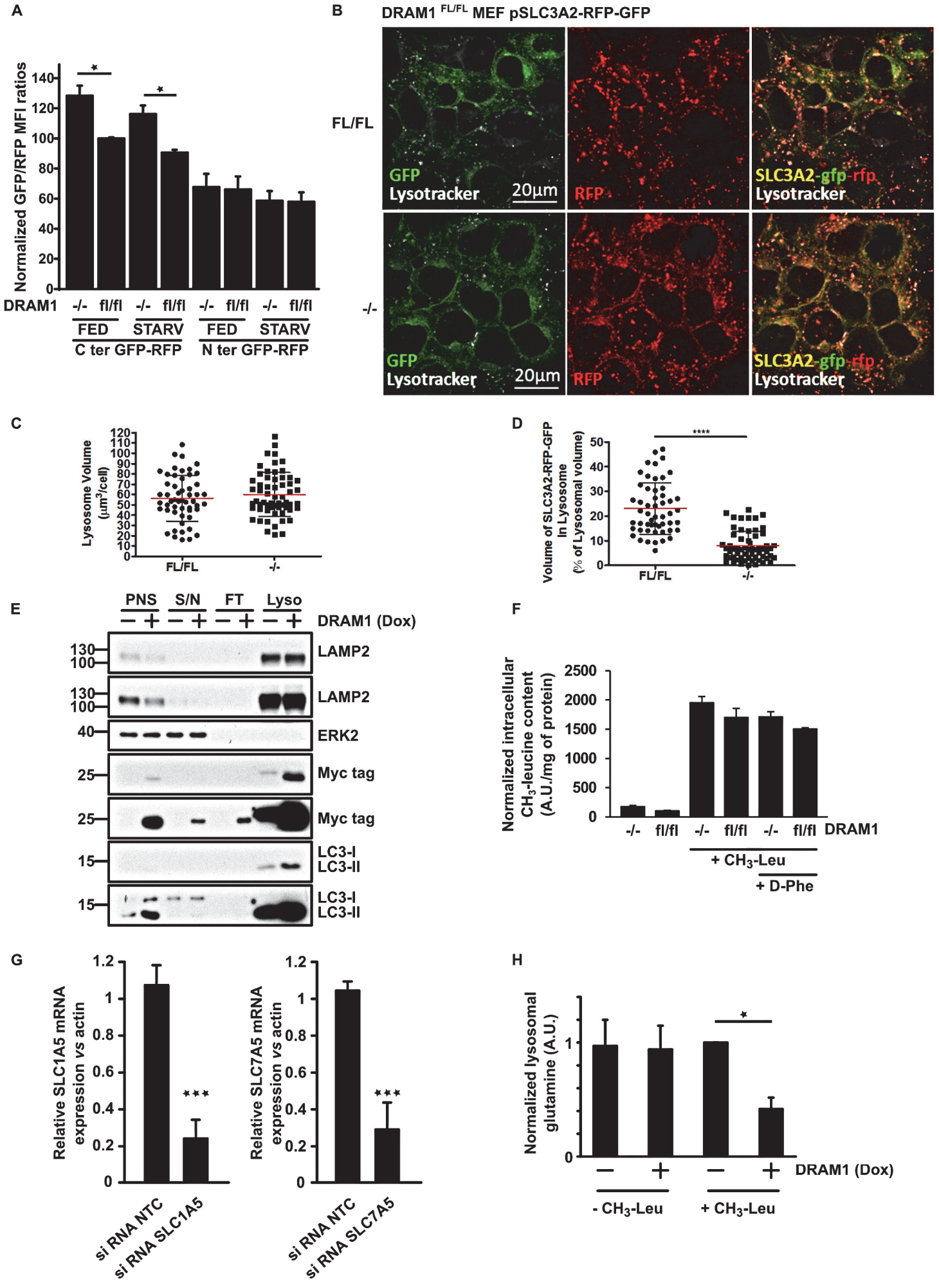

Beaumatin_Sup.Fig5

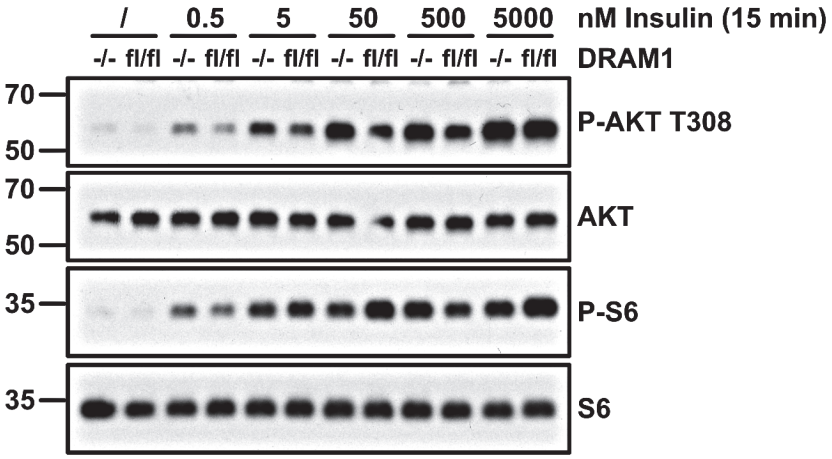

Beaumatin_Sup.Fig6

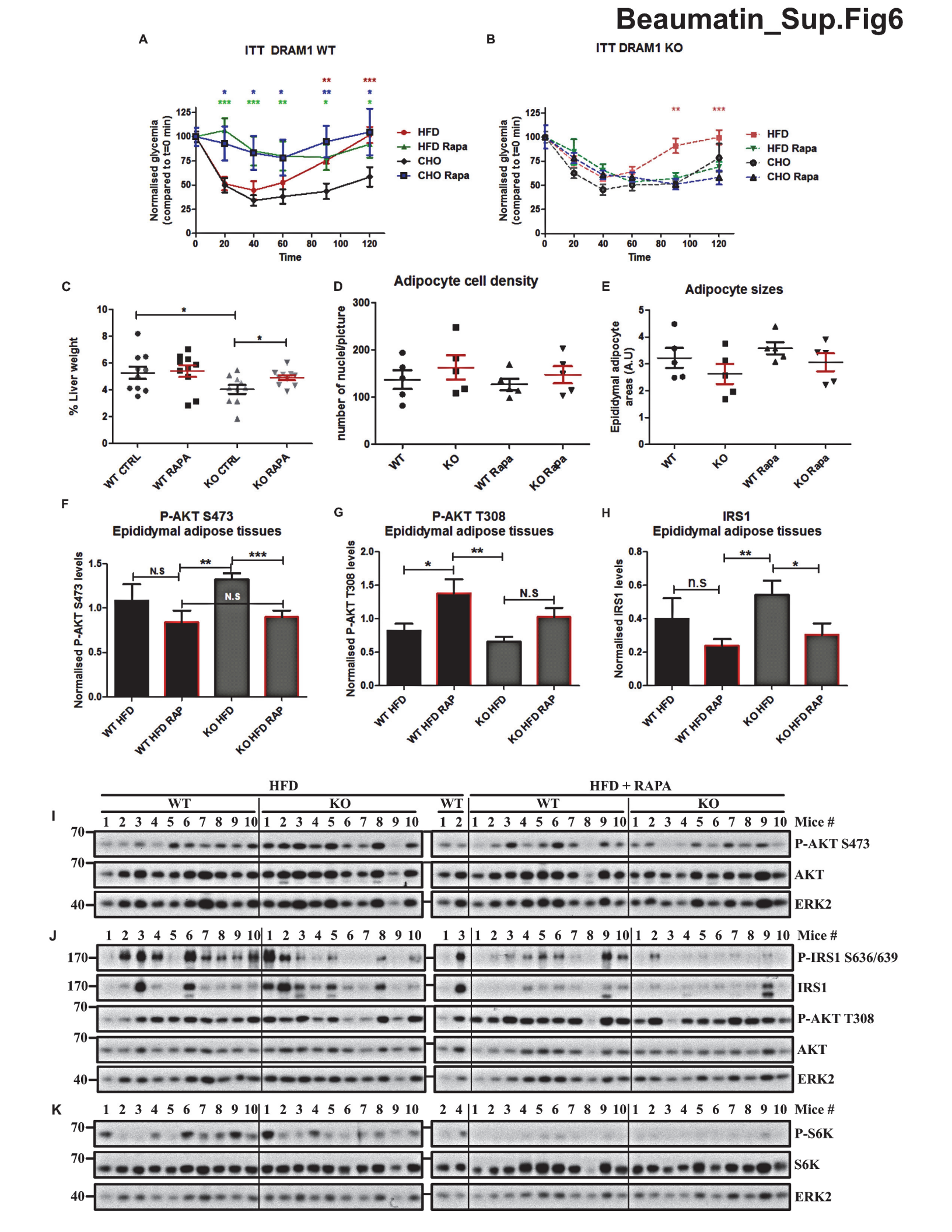

A

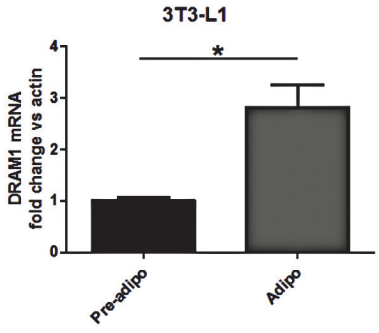
3T3-L1
DRAM1 mRNA fold change vs actin
*
Pre-adipo
Adipo

B

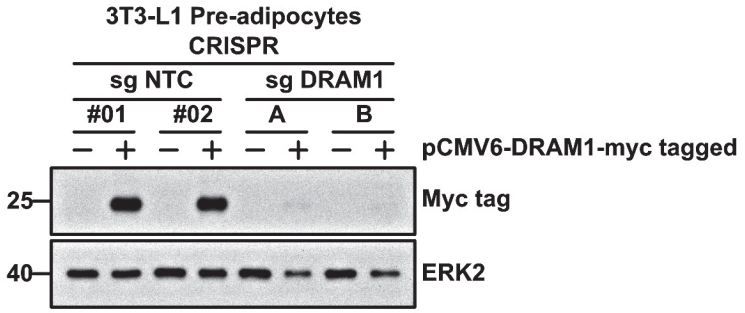
3T3-L1 Pre-adipocytes CRISPR
sg NTC
sg DRAM1
#01
#02
A
B
pCMV6-DRAM1-myc tagged
25
Myc tag
40
ERK2

C

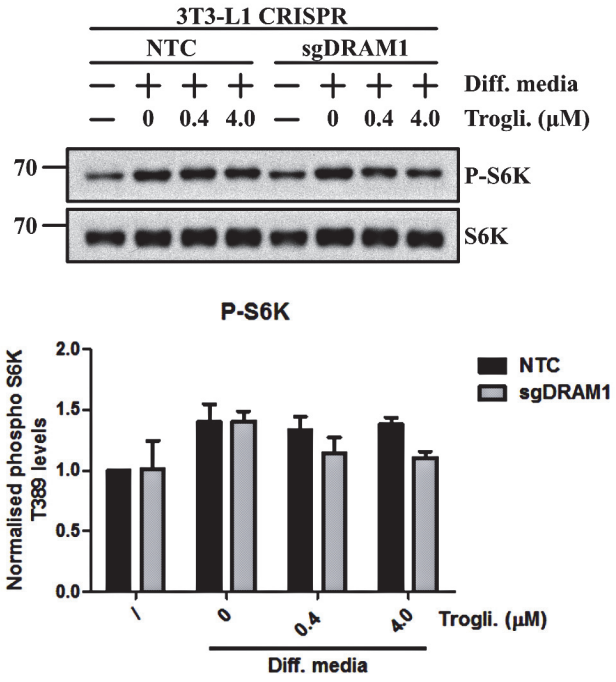
3T3-L1 CRISPR
NTC
sgDRAM1
Diff. media
Trogli. (µM)
70
P-S6K
70
S6K
P-S6K
Normalised phospho S6K T389 levels
NTC
sgDRAM1
Trogli. (µM)
Diff. media